Journal of Molecular Liquids 223 (2016) 1284–1290

Contents lists available at ScienceDirect

Journal of Molecular Liquids

journal homepage: www.elsevier.com/locate/molliq

Effects of MHD homogeneous-heterogeneous reactions on third grade fluid flow with Cattaneo-Christov heat flux

M. Ramzan[a,*], M. Bilal[b], Jae Dong Chung[c]

[a] Department of Computer Science, Bahria University, Islamabad Campus, Islamabad 44000, Pakistan
[b] Department of Mathematics, Faculty of Computing, Capital University of Science and Technology, Islamabad, Pakistan
[c] Department of Mechanical Engineering, Sejong University, Seoul 143-747, Republic of Korea

ARTICLE INFO

Article history:
Received 28 August 2016
Received in revised form 12 September 2016
Accepted 16 September 2016
Available online 24 September 2016

Keywords:
Homogenous-heterogeneous reactions
Cattaneo-Christov heat flux
MHD
Convective heat boundary condition

ABSTRACT

The present exploration discusses two dimensional incompressible third grade-fluid flow under the influence of Cattaneo-Christov heat flux and homogeneous-heterogeneous reactions. Effects of magneto-hydrodynamic and convective boundary condition are also taken into account. Boundary layer approach is engaged to obtain system of partial differential equations. Appropriate transformations are betrothed to transmute partial differential equations with high non-linearity to nonlinear differential equations. Renowned Homotopy Analysis method is summoned to find analytical solution of all involved distributions. Consequences of pertinent emerging parameters on related profiles are portrayed and relevant discussion is added with special focus on their physical aspects. It is observed that homogeneous and heterogeneous reactions depict conflicting behavior on Concentration distribution. It is also noted that increasing values of thermal relaxation parameter diminishes temperature field. A comparison to previous exploration is also added to validate our results.

1. Introduction

Non-Newtonian fluids are imperative in boundary layer flows because of their engineering and technology related applications. Apple sauce, tomato paste, paints, ketchup, polymeric liquids, jellies, glues, soaps, blood, inks, cosmetic products are examples of non-Newtonian fluids. As there are variety of non-Newtonian fluids so it is reasonably difficult to form an equation expressing the elastic and viscous properties of these fluids. In comparison to viscous fluids, mathematical modeling of non-Newtonian fluids is considerably complex and challenging. Even then many researchers are adding valuable contribution on these fluids highlighting different aspects [1–5] . Non-Newtonian fluids are categories as integral, differential and rate types. Second grade fluid which is a differential type fluid has the characteristics to identify normal stress differences only but shear thinning/thickening phenomena does not fall in its domain. Nevertheless, third-grade fluid model can predict about both features of shear thinning/thickening and normal stress. Many researchers have explored third grade fluid model with numerous aspects despite many complexities in its modeling. For example, Hayat et al. [6] found analytical solution of MHD third-grade fluid axisymmetric flow over a stretching cylinder using Homotopy Analysis method. Nadeem and Saleem [7] discussed flow of third grade nanofluid over vertical rotating cone with Homotopy Analysis method. Abbas et al. [8] examined third grade fluid flow near a stagnation point over a porous plate with chemical reaction. A hybrid numerical technique comprises of finite difference and shooting method is engaged. Third grade fluid flow with effect of Cattaneo-Christov heat flux over a surface which is stretched exponentially is studied by Shehzad et al. [9]. Javed and Mustafa [10] explored stagnation point third-grade fluid flow under the influence of mixed convection and viscous dissipation with slip boundary condition.

In nature, difference of temperature decides the rate of heat transfer between two bodies or within an independent unit. For the last two centuries, Fourier law of heat conduction has been the only yardstick to gauge heat transfer rate. One of the drawback of this law named “Paradox of heat conduction” was to generate parabolic energy equation which indicates that any disruption in the beginning will carry all through the substance. Cattaneo [11] addressed this candid problem by adding thermal relaxation time to Fourier law which transfer heat in the form of thermal waves with restricted speed. This model was improved by Christov [12] who

* Corresponding author.
E-mail address: mramzan@bahria.edu.pk (M. Ramzan).

http://dx.doi.org/10.1016/j.molliq.2016.09.046
0167-7322/

swapped Maxwell-Cattaneo's model time derivative by Oldroyd's upper-convected derivative to sanctuary its original formulation and documented as Cattaneo-Christov heat flux model in the literature. Distinctiveness of the solutions obtained from Cattaneo-Christov equations was verified by Ciarletta and Straughan [13]. Mustafa [14] found analytical solution of UMC fluid rotating flow with effect of Cattaneo-Christov heat flux. Abbasi et al. [15] examined Cattaneo–Christov heat flux model for incompressible Oldroyd-B fluid over a linearly stretching sheet using Optimal HAM. Rubab and Mustafa [16] found analytical solution of MHD three dimensional Maxwell fluid flow accompanying Cattaneo-Christov heat flux model using HAM. Shehzad et al. [17] discussed Cattaneo-Christov heat flux model in the flow of third-grade fluid past an exponential stretching sheet. A similar three dimensional Burger fluid study in attendance of Cattaneo-Christov heat flux model is conducted by Khan and Khan [18]. Some most recent attempts highlighting Cattaneo-Christov heat flux model are appended at Refs. [19–22].

A phase is a distinct, uniform state of a system that has no observable boundary which may divide the system into components. Chemical reactions are broadly classified into homogenous reactions (occurring in single phase) and heterogeneous reactions (involving multiple phases). A reaction is often aided with a catalyst, which enhances a reaction's rate by providing a substitute path for reaction having lower activation energy. In recent times, scientists are very much concerned in creating effective and efficient processes that includes an amalgamation of both homogenous and heterogeneous reactions; the researchers are currently much concerned with the study of the complex interactions of these reactions. Abbas et al. [23] discussed stagnation point fluid flow with of generalized slip condition under the influence of homogeneous–heterogeneous reactions past a permeable stretching surface using shooting method technique. Hayat et al. [24] found convergent series solution of viscoelastic fluid with effects of melting heat and homogeneous heterogeneous reactions due to a stretching cylinder. Hayat et al. [25] also investigated flow of two dimensional Oldroyd-B fluid under the influence of magnetohydrodynamic (MHD) and homogeneous–heterogeneous reactions using Homotopy Analysis method. Kameswaran et al. [26] explored homogeneous–heterogeneous reactions in a viscous nanofluid flow past a stretching sheet analytically when the auto catalyst and diffusion coefficients of the reactant are equal.

Convective heat transfer studies have gained significant consideration owing its applicability in different high temperature processes like nuclear power plants, gas turbines and storage of thermal energy etc. Recently, Ramzan et al. [27] discussed Micropolar fluid flow with effects of thermal radiation, joule heating and magnetohydrodynamic using Homotopy Analysis method. Haq et al. [28] debated convective heat transfer over a stretched surface in attendance of carbon nanotubes. They also incorporated effects of viscous dissipation and magnetohydrodynamic. Hayat et al. [29] examined effects of convective boundary condition on flow of nanoparticle in 3D Maxwell fluid flow. Hayat et al. [30] also explored nano particle concentration in the flow of couple stress fluid flow with convective boundary condition over a nonlinear stretched surface. Massod et al. [31] found numerical solution of stagnation point Carreau fluid flow with heat and mass convective boundary conditions under the influence of magnetohydrodynamic RK-method.

Motivation from above, the core objective of this investigation is to discuss flow of third grade fluid with effects and homogeneous-heterogeneous reaction and Cattaneo-Christov heat flux past a linear stretching sheet. Effects of convective boundary condition with magnetohydrodynamic are also taken into account. Analytical solution of problem is found using Homotopy Analysis method [32–37]. This seems to be a first attempt in this direction. Discussion of prominent parameters supported by graphs is added to the problem. Comparison with an earlier study is also featured in this exploration.

2. Mathematical formulation

We have considered MHD flow of third grade fluid under the combined effects of Cattaneo-Christov heat flux and homogeneous-heterogeneous reactions over a sheet stretched linearly along x-axis. Magnetic field of strength B_o is applied along $y-$axis. Induced magnetic field is ignored because of our supposition of small Reynolds number. Obviously, temperature at the sheet T_w is greater than the temperature far away from the sheet T_∞. There is an isothermal cubic autocatalytic (homogeneous) reaction on boundary layer flow however first order reaction (heterogeneous) is taken on catalyst surface that are represented by [23–26]

$$A + 2B \rightarrow 3B, \quad \text{rate} = k_c ab^2 \tag{1}$$

$$A \rightarrow B, \quad \text{rate} = k_s a \tag{2}$$

where k_c, k_s are rate constants and a, b are concentrations of the chemical species A, B respectively. Considering that there is no change in temperature for the both reactions. Employing boundary layer approximations and taking into account all considerations mentioned above, the governing equations of the system are

$$\frac{\partial u}{\partial x} + \frac{\partial v}{\partial y} = 0, \tag{3}$$

$$u\frac{\partial u}{\partial x} + v\frac{\partial u}{\partial y} = \nu\frac{\partial^2 u}{\partial y^2} + \frac{\alpha_1}{\rho}\left(u\frac{\partial^3 u}{\partial x \partial y^2} + \frac{\partial u}{\partial x}\frac{\partial^2 u}{\partial y^2} + v\frac{\partial^3 u}{\partial y^3} + 3\frac{\partial u}{\partial y}\frac{\partial^2 v}{\partial y^2}\right) + 2\frac{\alpha_2}{\rho}\frac{\partial u}{\partial y}\frac{\partial^2 u}{\partial y^2} + 6\frac{\beta_3}{\rho}\left(\frac{\partial u}{\partial y}\right)^2\frac{\partial^2 u}{\partial y^2} - \frac{\sigma B_o^2}{\rho}u, \tag{4}$$

$$\rho C_P\left(u\frac{\partial T}{\partial x} + v\frac{\partial T}{\partial y}\right) = -\nabla.\mathbf{q}, \tag{5}$$

$$u\frac{\partial a}{\partial x} + v\frac{\partial a}{\partial y} = D_A\frac{\partial^2 a}{\partial y^2} - k_c ab^2, \tag{6}$$

$$u\frac{\partial b}{\partial x} + v\frac{\partial b}{\partial y} = D_B\frac{\partial^2 b}{\partial y^2} + k_c ab^2, \tag{7}$$

where $\lambda_1, C_p, \nu, T, \alpha, \rho$ and q are retardation time, specific heat, kinematic viscosity, temperature, ratio of relaxation to retardation times, fluid density and heat flux respectively satisfying the equation

$$\mathbf{q} + \lambda_2\left(\frac{\partial \mathbf{q}}{\partial t} + \mathbf{V}.\nabla\mathbf{q} - \mathbf{q}.\nabla\mathbf{V} + (\nabla.\mathbf{V})\,\mathbf{q}\right) = -k\nabla T, \tag{8}$$

with k and λ_2 are fluid thermal conductivity and thermal relaxation time respectively. Ignoring $\mathbf{q}$ from Eqs. (5) and (8) with assumption by Christov [12], we get

$$u\frac{\partial T}{\partial x} + v\frac{\partial T}{\partial y} = \frac{k}{\rho C_P}\frac{\partial^2 T}{\partial y^2} - \lambda_2\left(\begin{array}{c} u^2\frac{\partial^2 T}{\partial x^2} + v^2\frac{\partial^2 T}{\partial y^2} + 2uv\frac{\partial^2 T}{\partial x \partial y} \\ + \left(u\frac{\partial u}{\partial x} + v\frac{\partial u}{\partial y}\right)\frac{\partial T}{\partial x} + \left(u\frac{\partial v}{\partial x} + v\frac{\partial v}{\partial y}\right)\frac{\partial T}{\partial y}\end{array}\right). \tag{9}$$

Subject to the boundary conditions

$$u = U_w = cx, \quad v = 0, -k\frac{\partial T}{\partial y} = h_f\left(T_w - T\right), \quad D_A\frac{\partial a}{\partial y} = k_s a, \quad D_B\frac{\partial b}{\partial y} = -k_s a, \text{at} \quad y = 0,$$

$$u \rightarrow 0, \quad a \rightarrow a_o, \quad b \rightarrow 0, T \rightarrow T_\infty \quad \text{as} y \rightarrow \infty, \tag{10}$$

where D_A, D_B and $a_0 > 0$ are diffusion coefficients and dimensional constant respectively. Moreover, U_w, k, T_w, h_f and $c\&a_o$ are velocity at wall, thermal conductivity of the fluid, wall temperature, heat transfer coefficient and dimensional constant respectively.

Using following transformations

$$u = cxf'(\eta), v = -\sqrt{c\nu}f(\eta), a = a_0 g(\eta),$$
$$\theta(\eta) = \frac{T - T_\infty}{T_w - T_\infty}, \eta = \sqrt{\frac{c}{\nu}}y, b = a_0 h(\eta). \tag{11}$$

Satisfaction of Eq. (3) is evident, however Eqs. (4),(6),(7),(9) and (10) lead to the following non-dimensional forms

$$f''' + ff'' - f'^2 + \epsilon_1\left(2f'f''' - ff'''' + 3f''^2\right) + 2\epsilon_2 f''^2 + 6\beta\,\mathrm{Re}\, f''^2 f''' - Mf' = 0, \tag{12}$$

$$g'' + Scfg' - Sck_1 gh^2 = 0, \tag{13}$$

$$\delta h'' + Scfh' + Sck_1 gh^2 = 0, \tag{14}$$

$$\theta'' + \mathrm{Pr} f\theta' - \mathrm{Pr}\,\gamma\left(f^2\theta'' + ff'\theta'\right) = 0, \tag{15}$$

$$f(0) = 0, f'(0) = 1, g'(0) = k_2 g(0), \delta h'(0) = -k_2 g(0),$$
$$\theta'(0) = -\gamma_1 (1 - \theta(0)), \text{at} \quad y = 0,$$
$$f'(\infty) \to 0, \quad g(\infty) \to 1, \theta(\infty) \to 0, \quad \text{as} \quad y \to \infty, \tag{16}$$

where $(\epsilon_1, \epsilon_2, \beta), \gamma, Sc, Pr, \delta, M, \mathrm{Re}$ and (k_1, k_2) are the material parameters for third grade fluid, thermal relaxation time, Schmidt number, Prandtl number, ratio of diffusion coefficient, Hartmann number, Reynold number and amount of homogenous and heterogeneous reactions respectively. These quantities are demarcated as stated below

$$\mathrm{Pr} = \frac{\mu C_p}{k}, \quad \beta = \frac{\beta_3 U_w^3}{\rho\nu^2 x}, \quad \gamma = \lambda_2 c, \quad S = \frac{Q}{\rho a C_p}, k_1 = \frac{k_c a_0^2}{c},$$
$$\delta = \frac{D_B}{D_A}, M = \frac{\sigma B_o^2}{\rho c}, \gamma_1 = \frac{h_f}{k}\sqrt{\frac{\nu}{a}}, M = \frac{\sigma B_o^2}{a\rho}, Sc = \frac{\nu}{D_A}, k_2 = \frac{k}{D_A a_0}\sqrt{\frac{c}{\nu}},$$
$$\epsilon_1 = \frac{\alpha_1 c}{\rho\nu}, \epsilon_2 = \frac{\alpha_2 c}{\rho\nu}. \tag{17}$$

With the assumption that diffusion coefficients of chemical species A and B are of analogous magnitude and this lead us to suppose that D_A and D_B are identical provided $\delta = 1$. Thus, we have

$$g(\eta) + h(\eta) = 1. \tag{18}$$

From this, Eqs. (13) and (14) take the form

$$g'' + Scfg' - Sck_1 g(1 - g)^2 = 0, \tag{19}$$

and respective boundary conditions eventually come to the following form

$$g'(0) = k_2 g(0), \quad g(\infty) = 1. \tag{20}$$

Skin friction coefficient and local Nusselt number in dimensional form are

$$C_{fx} = \frac{\tau_w}{\frac{\rho}{2}u_w^2(x)}, \quad Nu_x = \frac{xq_w}{k(T_w - T_\infty)}, \tag{21}$$

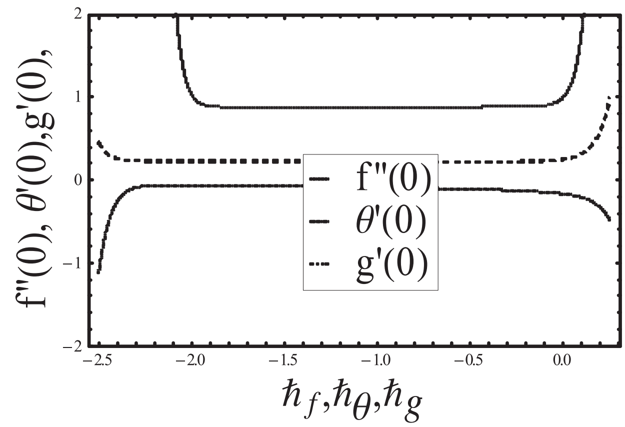

Fig. 1. Graph of f, θ and g.

where τ_w and q_w are the sheer stress and surface heat flux are

$$\tau_w = \left[\mu_0\frac{\partial u}{\partial y} + \alpha_1\left(u\frac{\partial^2 u}{\partial x\partial y} + v\frac{\partial^2 u}{\partial y^2} + 2\frac{\partial u}{\partial x}\frac{\partial u}{\partial y}\right) + 2\frac{\beta_3}{\rho}\left(\frac{\partial u}{\partial y}\right)^3\right]_{y=0}.$$
$$q_w = -k\left(\frac{\partial T}{\partial y}\right)_{y=0}. \tag{22}$$

Dimensionless forms of skin friction coefficient and local Nusselt number are represented by

$$\frac{C_{fx}Re_x^{1/2}}{2} = \left[f''(0) + \epsilon_1\{f'(0)f''(0) - f(0)f'''(0)\}\right] + 2\beta \quad \mathrm{Re}f''^3(0)\Big],$$
$$N_{u_x}Re_x^{-1/2} = -\theta'(0). \tag{23}$$

3. Homotopic Analysis solutions

Analytical solutions for the derived system of equations with associated boundary conditions are obtained using Homotopy Analysis method (HAM). In this specific method or other technique, initial guesses are necessitated whenever series solution is required. Considering boundary conditions Eq. (16) and semi-infinite domain of our problem, choice of initial guesses of the form $e^{-\eta}$ will give a rapid convergence whenever $\eta \to \infty$. That is why we select initial guesses $(f_0(\eta), g_0(\eta), \theta_0(\eta))$ and respective operators $(\mathcal{L}_f(\eta), \mathcal{L}_g(\eta), \mathcal{L}_\theta(\eta))$ as given below

$$f_0(\eta) = 1 - e^{-\eta}, g_0(\eta) = 1 - \frac{e^{-k_2\eta}}{2}, \theta_0(\eta) = \frac{\gamma_1}{1 + \gamma_1}e^{-\eta}, \tag{24}$$

$$\mathcal{L}_f(\eta) = f''' - f', \quad \mathcal{L}_g(\eta) = g'' - g', \mathcal{L}_\theta(\eta) = \theta'' - \theta'. \tag{25}$$

These operators own the following properties

$$\mathcal{L}_f\left[C_1 + C_2e^{\eta} + C_3e^{-\eta}\right] = 0, \tag{26}$$

$$\mathcal{L}_g\left[C_4e^{\eta} + C_5e^{-\eta}\right] = 0, \tag{27}$$

$$\mathcal{L}_\theta\left[C_6e^{\eta} + C_7e^{-\eta}\right] = 0, \tag{28}$$

Table 1
Convergence of Homotopic solutions for various order of estimates when $\alpha = 0.2, \beta = 0.3, M = 0.3, \mathrm{Pr} = 1.0, \gamma = \mathrm{Re} = 0.1, \gamma_1 = 0.2, > Sc = 1.0, k_1 = 0.2, > k_0 = 0.2, k = 0.4$.

Order of approximations	$-f''(0)$	$-\theta'(0)$	$-g'(0)$
1	1.03667	0.19730	−0.16317
5	1.06528	0.19318	−0.15580
10	1.07157	0.19297	−0.15228
15	1.07343	0.19391	−0.15069
20	1.07420	0.19505	−0.14982
25	1.07459	0.19616	−0.14930
30	1.07493	0.19720	−0.14896
35	1.07495	0.19814	−0.14872
40	1.07495	0.19814	−0.14872

where $C_i (i = 1 - 9)$ are the arbitrary constants. Through boundary conditions, the values of these constants are given by

$$C_2 = C_4 = C_6 = 0, C_3 = \left.\frac{\partial f_m^\star(\eta)}{\partial \eta}\right|_{\eta=0}, C_1 = -C_3 - f_m^\star(0),$$
$$C_5 = \frac{1}{1+k_2}\left(\left.\frac{\partial g_m^\star(\eta)}{\partial \eta}\right|_{\eta=0} - k_2 g_m^\star(0)\right),$$
$$C_7 = \frac{1}{1+\gamma_1}\left(\left.\frac{\partial \theta_m^\star(\eta)}{\partial \eta}\right|_{\eta=0} - \gamma_1 \theta_m^*(0)\right). \quad (29)$$

4. Convergence analysis and discussion

Auxiliary parameters play a fundamental role to standardize convergence of solutions in series form. In HAM, the accurate selection of these parameters is fundamental to regulate the convergence of solutions. To pick apposite values of auxiliary parameters $\hbar_f$, $\hbar_\theta$ and $\hbar_g$, $\hbar$-curves are plotted to 20th order of approximations. Fig. 1 shows that acceptable values of auxiliary parameters $\hbar_f$, $\hbar_\theta$ and $\hbar_g$ are $-1.8 \le \hbar_f \le -0.4, -2.1 \le \hbar_\theta \le -0.5$ and $-2.0 \le \hbar_g \le -0.4$. Table 1 displays that 35th order of approximations are acceptable for series solution to converge for velocity, temperature and concentration profiles. Fig. 2 is plotted to observe the behavior of third grade parameter β on velocity distribution. Increasing values of β boosts the sheer thinning which eventually results in increasing velocity profile. From Fig. 3, it is evident that temperature distribution is decreasing function of material parameter ϵ_1. Growing values of material parameter corresponds to vigorous viscoelasticity. Sturdy values of viscoelasticity causes reduction in temperature field. Fig. 4 evidently specifies that both temperature field and its associated boundary layer thickness are enriched with higher values of Hartmann number M. Hartmann number has a direct proportionate with Lorentz force. A fluid with mounting values of Hartmann number has sturdier Lorentz force. Because of robust Lorentz force, temperature and its allied boundary layer thickness are increased for higher values of Hartmann number. It is perceived from Fig. 5 that temperature and its related boundary layer thickness are abridged for higher values of Prandtl number Pr. A ratio of viscous to thermal diffusivity is recognized as Prandtl number. A weaker thermal diffusivity is encountered for larger Prandtl number and vice versa. This reigning causes reduction in temperature distribution. Fig. 6 depicts impact of Biot number γ_1 on temperature profile. It is clear from the graph that temperature field is mounting function of Biot number. Biot number has dependency on heat transfer coefficient. Large values of heat transfer coefficient lead to higher temperature. That is why high temperature distribution is observed for increasing values of Biot number. In Fig. 7 effect of k_1 (amount of forte of homogeneous reaction) on concentration profile is portrayed. As the reactants are used up in a chemical reaction. Because of this fact concentration

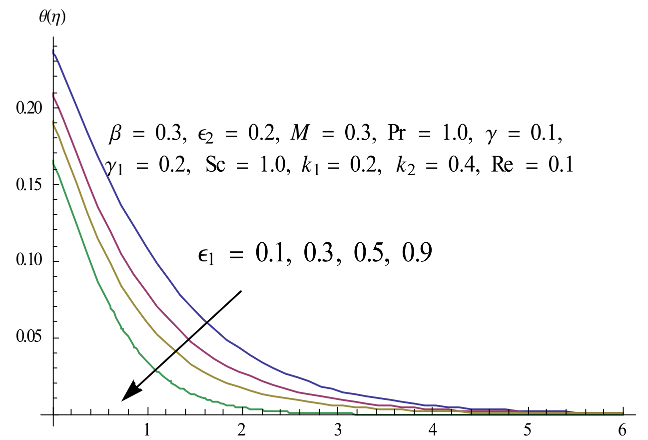

Fig. 3. Graph of $\theta(\eta)$ versus η for different values of ϵ_1.

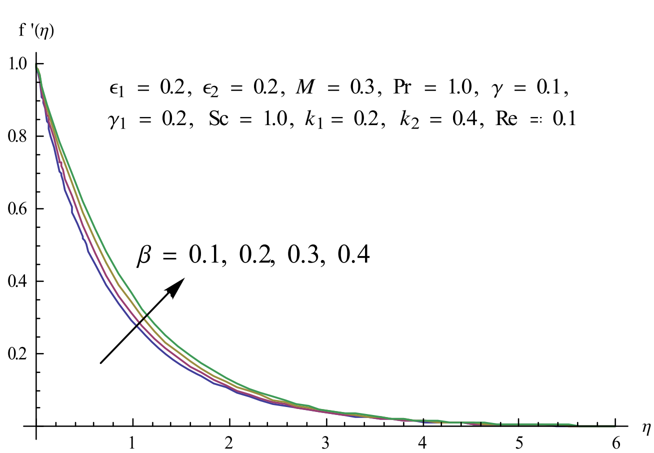

Fig. 2. Graph of $f'(\eta)$ versus η for different values of β.

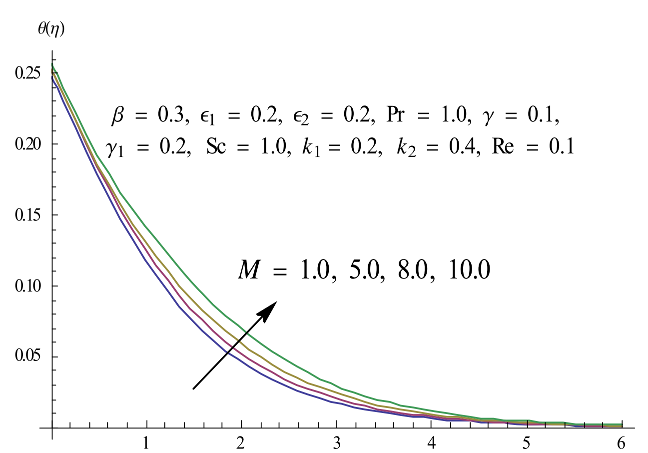

Fig. 4. Graph of $\theta(\eta)$ versus η for different values of M.

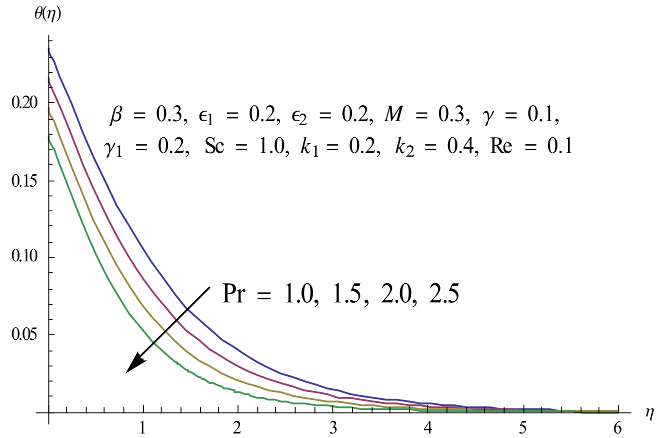

Fig. 5. Graph of $\theta(\eta)$ versus η for different values of Pr.

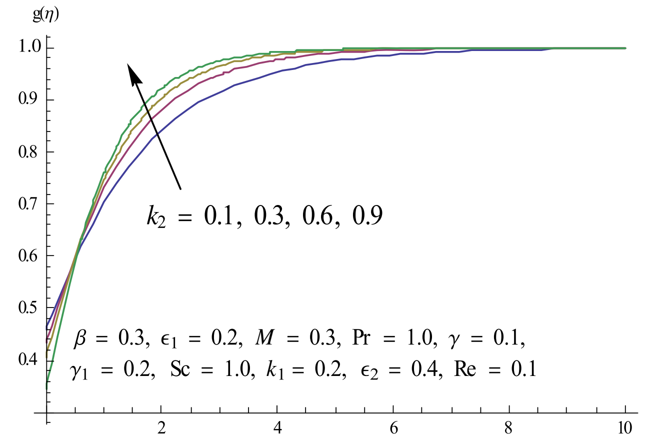

Fig. 8. Graph of $g(\eta)$ versus η for different values of k_2.

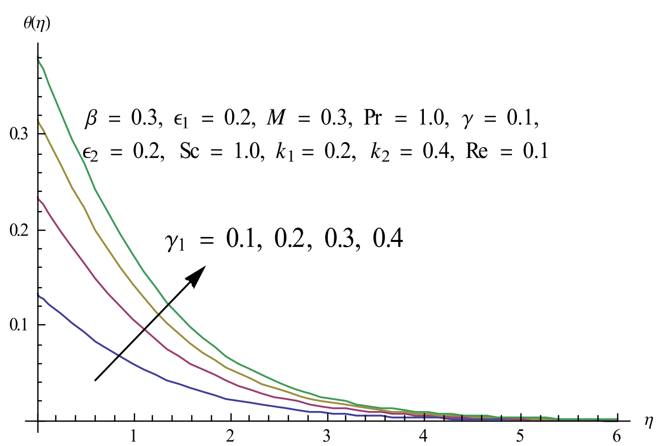

Fig. 6. Graph of $\theta(\eta)$ versus η for different values of γ_1.

field shows decreasing tendency for larger values of k_1. From Fig. 8, it is evident that concentration distribution is increasing function of k_2 (amount of forte of the heterogeneous reaction). Higher values of k_2 weaken diffusion coefficient and as a result less diffused particles strengthen the concentration field. Influence of Schmidt number *Sc* on $g(\eta)$ is given in Fig. 9. It is noted that concentration field is an growing function of Schmidt number. The quotient of momentum diffusivity to mass diffusivity is known as Schmidt number. Higher Schmidt number corresponds to high momentum diffusivity which in turn increases the concentration distribution. In order to analyze the heat transfer rate and friction of fluid in the vicinity of the surface, results are plotted for local Nusselt number and skin friction with respect to the various values of emerging physical parameters (see Figs. 10 and 11). Since the Prandtl number is the ratio of dynamic viscosity to the thermal diffusivity, so when we raise the values of Prandtl number then fluid molecules diffuse and consequently energy will lose. The same situation arises in Fig. 10 for local Nusselt number with respect to the different values of *Pr*. On the other hand, Nusselt number slightly varies due to increasing values of Biot number. Fig. 11 demonstrates the simultaneous effects of third grad parameter and Hartmann number. As per physical phenomena, highly viscous fluid leads to enhance the tendency of drag with the surface, so when we increase the values of non-Newtonian parameter gives the rise in the skin friction coefficient and these results can be verified via Fig. 11. To control the random motion of fluid particles magnetic strength is applied in the normal direction at the surface of the sheet. One can find the Hartmann number leads to control the motion of fluid particles and restricts that random motion of the particles in uniform manners. As a result friction with the surface of the sheet decreases with increasing values

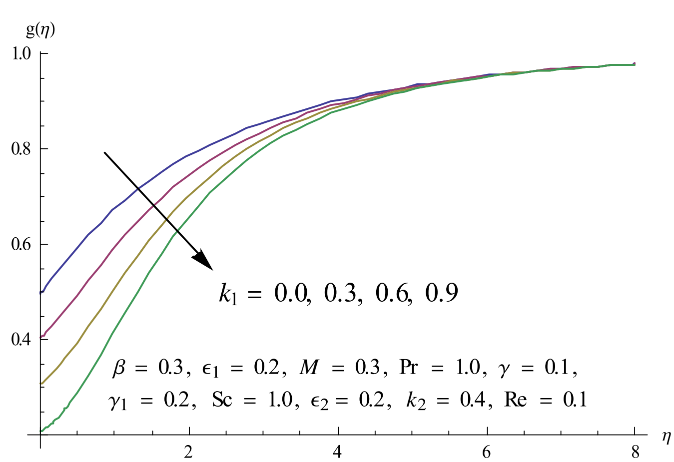

Fig. 7. Graph of $g(\eta)$ versus η for different values of k_1.

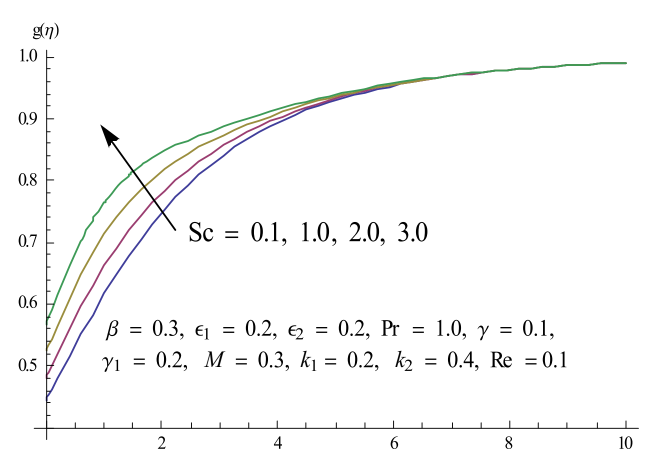

Fig. 9. Graph of $g(\eta)$ versus η for different values of *Sc*.

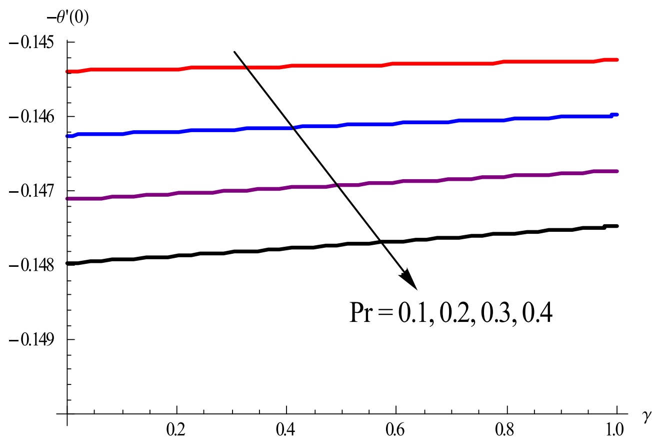

Fig. 10. Graph of Nusselt number versus γPr.

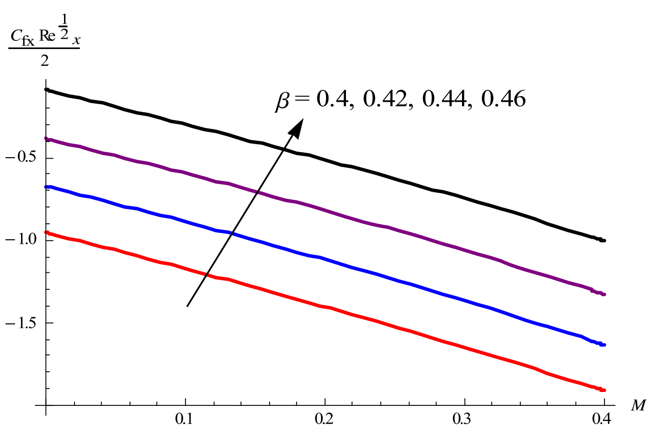

Fig. 11. Graph of Skin friction versus M versus β.

of M. Fig. 12 portrays impact of thermal relaxation parameter γ on temperature profile. It is perceived that snowballing values of thermal relaxation parameter diminishes temperature profile. Additional time is prerequisite for transmission of heat to adjacent particles if thermal relaxation parameter is given escalating values. This fact reveals that mounting values of thermal relaxation parameter casts an insulated material which is accountable for declining temperature field. If we make $\gamma = 0$, heat will transfer swiftly through the material. That is why temperature field is stronger if $\gamma = 0$ in case

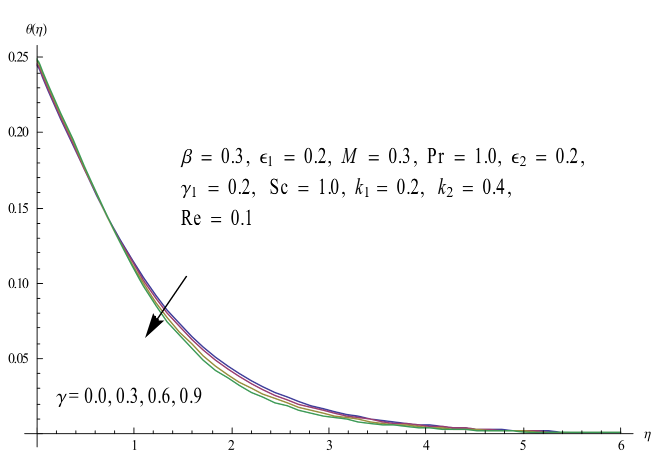

Fig. 12. Graph of $\theta(\eta)$ versus η for different values of γ.

Table 2
Comparison of $C_{fx}Re_x^{1/2}$ for varied values.

ϵ_1	ϵ_2	β	M	Re	Hayat et al. [37]	Present
0.00	0.2	0.2	0.10	0.70	1.453	1.453
0.10					1.532	1.533
0.14					1.567	1.566
0.10	0.00	0.2	0.10	0.70	1.600	1.600
	0.10				1.632	1.632
	0.20				1.668	1.667
0.10	0.10	0.00	0.10	0.70	1.433	1.432
		0.10			1.489	1.489
		0.20			1.532	1.532
0.10	0.10	0.2	0.1	0.70	1.532	1.532
			0.2		1.536	1.535
			0.3		1.545	1.545
0.10	0.10	0.2	0.1	0.7	1.532	1.532
				0.8	1.542	1.542
				0.9	1.551	1.552

of Fourier Law in comparison to Cattaneo-Christov heat flux model. Table 2 represents numerical values of Skin friction coefficient compared with earlier published work [37] and results are found in good agreement.

5. Final remarks

We in this paper have investigated effects of homogeneous-heterogeneous reactions, magnetohydrodynamic and Cattaneo-Christov heat flux on two dimensional third grade fluid with convective boundary condition. Homotopy Analysis is summoned to address system of equations with high nonlinearity. The main findings of present investigation are summarized as given below:

- Homogeneous and heterogeneous reactions show opposing behavior on Concentration distribution.
- Temperature field is growing function of Biot number.
- Prandtl number and thermal relaxation time show opposite tendency on local Nusselt number.
- Increasing values of Hartmann number boosts temperature and its allied boundary layer thickness.
- Temperature distribution is decreasing function of thermal relaxation parameter.

Conflict of Interest

Authors have no conflict of interest regarding this publication.

Acknowledgments

This research is supported by Korea Institute of Energy Technology Evaluation and Planning (KETEP) granted financial resource from the Ministry of Trade, Industry & Energy of Korea (No. 20132010101780).

References

[1] K. Ahmad, Z. Hanouf, A. Ishak, Mixed convection Jeffrey fluid flow over an exponentially stretching sheet with magnetohydrodynamic effect, AIP Adv. 6 (2016) 035024.
[2] M. Ramzan, M. Farooq, T. Hayat, J.D. Chung, Radiative and Joule heating effects in the MHD flow of a micropolar fluid with partial slip and convective boundary condition, J. Mol. Liq. 221 (2016) 394–400.
[3] M. Ramzan, M. Farooq, M.S. Alhothuali, H.M. Malaikah, W. Cui, T. Hayat, Three dimensional flow of an Oldroyd-B fluid with Newtonian heating, Int. J. Numer. Methods Heat Fluid Flow 25 (1) (2015) 68–85.

[4] T. Hayat, Z. Hussain, A. Alsaedi, M. Farooq, Magnetohydrodynamic flow by a stretching cylinder with Newtonian heating and homogeneous-heterogeneous reactions, PLoS ONE 11 (6). (2016) e0156955.

[5] M. Ramzan, F. Yousaf, M. Farooq, J.D. Chung, Mixed convective viscoelastic nanofluid flow past a porous media with Soret-Dufour effects, Commun. Theor. Phys. 66 (2016) 133–142.

[6] T. Hayat, A. Shafiq, A. Alsaedi, MHD Axisymmetric flow of third grade fluid by a stretching cylinder, Alexandria Eng. J. 54 (2) (2015) 205–212.

[7] S. Nadeem, S. Saleem, Analytical study of third grade fluid over a rotating vertical cone in the presence of nanoparticles, Int. J. Heat Mass Transf. 85 (2015) 1041–1048.

[8] Z. Abbas, T. Javed, N. Ali, M. Sajid, Diffusion of chemically reactive species in stagnation-point flow of a third grade fluid: a hybrid numerical method, J. Appl. Fluid Mech. 9 (1) (2016) 195–203.

[9] S.A. Shehzad, F.M. Abbasi, T. Hayat, B. Ahmad, Cattaneo-Christov heat flux model for third-grade fluid flow towards exponentially stretching sheet, Appl. Math. Mech. 37 (6) (2016) 761–768.

[10] T. Javed, I. Mustafa, Slip effects on a mixed convection flow of a third-grade fluid near the orthogonal stagnation point on a vertical surface, J. Appl. Mech. Tech. Phys. 57 (3) (2016) 527–536.

[11] C. Cattaneo, Sulla Conduzionedelcalore, Atti Del Seminario Matematico E Fisico Dell Università Di Modena E Reggio Emilia, 3. 1948, 83–101.

[12] C.I. Christov, On frame indifferent formulation of the Maxwell-Cattaneo model of finite-speed heat conduction, Mech. Res. Commun. 36 (2009) 481–486.

[13] M. Ciarletta, B. Straughan, Uniqueness and structural stability for the Cattaneo-Christov equations, Mech. Res. Commun. 37 (2010) 445–447.

[14] M. Mustafa, Cattaneo-Christov heat flux model for rotating flow and heat transfer of upper-convected Maxwell fluid, AIP Adv. 5 (2015) 047109.

[15] F.M. Abbasi, M. Mustafa, S.A. Shehzad, M.S. Alhuthali, T. Hayat, Analytical study of Cattaneo-Christov heat flux model for a boundary layer flow of Oldroyd-b fluid, Chin. Phys. B 25 (2016) 1.

[16] K. Rubab, M. Mustafa, Cattaneo-Christov heat flux model for MHD three-dimensional flow of maxwell fluid over a stretching sheet, PLoS ONE 11 (2016) 4.

[17] S.A. Shehzad, F.M. Abbasi, T. Hayat, B. Ahmad, Cattaneo-Christov heat flux model for third-grade fluid flow towards exponentially stretching sheet, Appl. Math. Mech. 37 (6) (2016) 761–768.

[18] M. Khan, W.A. Khan, Three-dimensional flow and heat transfer to burgers fluid using Cattaneo-Christov heat flux model, J. Mol. Liq. 221 (2016) 651–657.

[19] M. Waqas, T. Hayat, M. Farooq, S.A. Shehzad, A. Alsaedi, Cattaneo-Christov heat flux model for flow of variable thermal conductivity generalized Burgers fluid, J. Mol. Liq. 220 (2016) 642–648.

[20] T. Hayat, M.I. Khan, M. Farooq, A. Alsaedi, M. Waqas, T. Yasmeen, Impact of Cattaneo-Christov heat flux model in flow of variable thermal conductivity fluid over a variable thicked surface, Int. J. Heat Mass Transf. 99 (2016) 702–710.

[21] M. Mustafa, Cattaneo-Christov heat flux model for rotating flow and heat transfer of upper-convected Maxwell fluid, AIP Adv. 5 (2015) 047109.

[22] F.M. Abbasi, S.A. Shehzad, Heat transfer analysis for three-dimensional flow of Maxwell fluid with temperature dependent thermal conductivity: application of Cattaneo-Christov heat flux model, J. Mol. Liq. 220 (2016) 848–854.

[23] Z. Abbas, M. Sheikh, I. Pop, Stagnation-point flow of a hydromagnetic viscous fluid over stretching/shrinking sheet with generalized slip condition in the presence of homogeneous-heterogeneous reactions, J. Taiwan Inst. Chem. Eng. 55 (2015) 69–75.

[24] T. Hayat, Z. Hussain, M. Farooq, A. Alsaedi, Effects of homogeneous and heterogeneous reactions and melting heat in the viscoelastic fluid flow, J. Mol. Liq. 215 (2016) 749–755.

[25] T. Hayat, M. Imtiaz, A. Alsaedi, S. Almezal, On Cattaneo-Christov heat flux in MHD flow of Oldroyd-B fluid with homogeneous-heterogeneous reactions, J. Magn. Magn. Mater. 401 (2016) 296–303.

[26] P.K. Kameswaran, S. Shaw, P. Sibanda, P.V.S.N. Murthy, Homogeneous-heterogeneous reactions in a nanofluid flow due to a porous stretching sheet, Int. J. Heat Mass Transf. 57 (2) (2013) 465–472.

[27] M. Ramzan, M. Farooq, T. Hayat, J.D. Chung, Radiative and joule heating effects in the MHD flow of a micropolar fluid with partial slip and convective boundary condition, J. Mol. Liq. 221 (2016) 394–400.

[28] R.U. Haq, S. Nadeem, Z.H. Khan, N.F.M. Noor, Convective heat transfer in MHD slip flow over a stretching surface in the presence of carbon nanotubes, Physica B 457 (2015) 40–47.

[29] T. Hayat, T. Muhammad, S.A. Shehzad, G.Q. Chen, I.A. Abbas, Interaction of magnetic field in flow of Maxwell nanofluid with convective effect, J. Magn. Magn. Mater. 389 (2015) 48–55.

[30] T. Hayat, A. Aziz, T. Muhammad, B. Ahmad, Influence of magnetic field in three--dimensional flow of couple stress nanofluid over a nonlinearly stretching surface with convective condition, PLoS ONE 10 (12). (2015) e0145332.

[31] Hashim, M. Khan, A.S. Alshomrani, MHD stagnation-point flow of a Carreau fluid and heat transfer in the presence of convective boundary conditions, PLoS ONE 11 (6). (2016) e0157180.

[32] M. Ramzan, M. Bilal, Three-dimensional flow of an elastico-viscous nanofluid with chemical reaction and magnetic field effects, J. Mol. Liq. 215 (2016) 212–220.

[33] S.A. Shehzad, T. Hussain, T. Hayat, M. Ramzan, A. Alsaedi, Boundary layer flow of third grade nanofluid with Newtonian heating and viscous dissipation, J. Cent. South Univ. 22 (1) (2015) 360–367.

[34] T. Hussain, S.A. Shehzad, T. Hayat, A. Alsaedi, F. Solamy, M. Ramzan, Radiative hydromagnetic flow of Jeffrey nanofluid by an exponentially stretching sheet, PLoS ONE 9 (8). (2014) e103719.

[35] M. Ramzan, F. Yousaf, Boundary layer flow of three-dimensional viscoelastic nanofluid past a bi-directional stretching sheet with Newtonian heating, AIP Adv. 5 (5). (2015) 057132.

[36] M. Ramzan, Influence of Newtonian heating on three dimensional MHD flow of couple stress nanofluid with viscous dissipation and joule heating, PLoS ONE 10 (4). (2015) e0124699.

[37] T. Hayat, A. Shafiq, A. Alsaedi, Effect of joule heating and thermal radiation in flow of third grade fluid over radiative surface, PLoS ONE 9 (1) (2014) e83153.